molecular pharmaceutics

Article

pubs.acs.org/molecularpharmaceutics

Neuronal Uptake and Neuroprotective Properties of Curcumin-Loaded Nanoparticles on SK-N-SH Cell Line: Role of Poly(lactide-*co*-glycolide) Polymeric Matrix Composition

Ghislain Djiokeng Paka,[†,‡] Sihem Doggui,[†] Ahlem Zaghmi,[†] Ramia Safar,[§] Lé Dao,[⊥] Andreas Reisch,[¶] Andrey Klymchenko,[¶] V. Gaëlle Roullin,[∥] Olivier Joubert,[§] and Charles Ramassamy*[,†,‡]

[†]INRS-Institut Armand Frappier, 531 Boulevard des Prairies, Laval, Quebec H7V 1B7, Canada

[‡]INAF, Laval University, Québec G1V 0A6, Canada

[§]Faculté de Pharmacie, EA3452 CITHEFOR, Université de Lorraine, 54000 Nancy, France

[⊥]INRS-EMT, Québec H5A 1K6, Canada

[¶]Laboratoire de Biophotonique et Pharmacologie, Faculté de Pharmacie, Université de Strasbourg, 67081 Strasbourg, France

[∥]Laboratoire de Nanotechnologies Pharmaceutiques, Faculté de Pharmacie, Université de Montréal, Montréal H3T 1J4, Canada

ABSTRACT: Curcumin, a neuroprotective agent with promising therapeutic approach has poor brain bioavailability. Herein, we demonstrate that curcumin-encapsulated poly(lactide-*co*-glycolide) (PLGA) 50:50 nanoparticles (NPs-Cur 50:50) are able to prevent the phosphorylation of Akt and Tau proteins in SK-N-SH cells induced by H_2O_2 and display higher anti-inflammatory and antioxidant activities than free curcumin. PLGA can display various physicochemical and degradation characteristics for controlled drug release applications according to the matrix used. We demonstrate that the release of curcumin entrapped into a PLGA 50:50 matrix (NPs-Cur 50:50) is faster than into PLGA 65:35. We have studied the effects of the PLGA matrix on the expression of some key antioxidant- and neuroprotective-related genes such as APOE, APOJ, TRX, GLRX, and REST. NPs-Cur induced the elevation of GLRX and TRX while decreasing APOJ mRNA levels and had no effect on APOE and REST expressions. In the presence of H_2O_2, both NPs-Cur matrices are more efficient than free curcumin to prevent the induction of these genes. Higher uptake was found with NPs-Cur 50:50 than NPs-Cur 65:35 or free curcumin. By using PLGA nanoparticles loaded with the fluorescent dye Lumogen Red, we demonstrated that PLGA nanoparticles are indeed taken up by neuronal cells. These data highlight the importance of polymer composition in the therapeutic properties of the nanodrug delivery systems. Our study demonstrated that NPs-Cur enhance the action of curcumin on several pathways implicated in the pathophysiology of Alzheimer's disease (AD). Overall, these results suggest that PLGA nanoparticles are a promising strategy for the brain delivery of drugs for the treatment of AD.

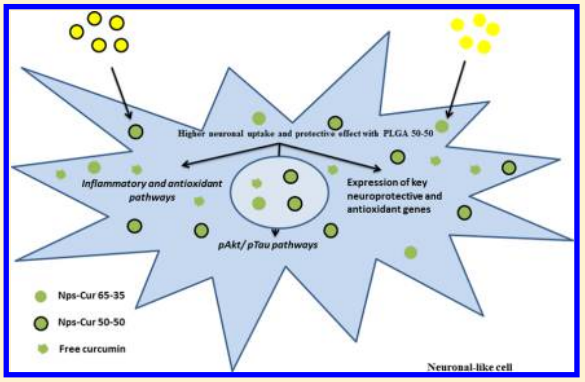

KEYWORDS: *nanoformulation, curcumin, oxidative stress, tau hyperphosphorylation, neuroprotective genes*

INTRODUCTION

Alzheimer's disease (AD) is one of the most common forms of dementia.[1] Because of the aging of the population, AD has become one of the most severe, progressive, socio-economical and medical burden all over the world.[2] The current treatment can cause severe side effects, which often cause the discontinuation of these pharmacotherapies.[3] Moreover, only 25−50% of patients respond to these therapies.[4] Therefore, the development of novel strategies to treat AD remains a great challenge.

The physiopathology of AD is multifactorial and implicates the deregulation of numerous molecular pathways such as the β-amyloid cascade, tau-phosphorylation, inflammation, and oxidative stress in the brain.[5] Indeed, it is well established that oxidative stress can induce neuronal cell death and neurodegeneration.[6−8] Interestingly, data obtained from patients with mild cognitive impairment (MCI), a preclinical stage of AD, strongly suggest that oxidative stress represents a major determinant of the pathogenesis and progression of AD.[9−11] This notion is strengthened by data obtained from transgenic mice models of AD.[12]

Curcumin is a hydrophobic polyphenolic compound widely considered as an effective therapy for several pathological conditions including asthma, epilepsy, gall stone, diabetic wound healing, and cancer.[13] The hypothesis of a potential

Received: August 7, 2015
Revised: October 27, 2015
Accepted: November 30, 2015
Published: November 30, 2015

DOI: 10.1021/acs.molpharmaceut.5b00611
Mol. Pharmaceutics 2016, 13, 391−403

therapeutic application of curcumin in dementia originates from epidemiological data and thereafter experimental data that point out its antioxidant, antiinflammatory, and neuroprotective properties. Synoptically, because of pleiotropic actions of curcumin, several actual and ongoing clinical trials deal with the overall action of curcumin or derivatives for numerous applications including neuroprotection. Accumulating data have demonstrated its neuroprotective property through antioxidant, anti-inflammatory, antiamyloid, antitau hyperphosphorylation, and metal chelation activities[14−17] (also see review in ref 18). We have recently demonstrated that curcumin protects neuronal cells against acrolein-induced toxicity by reducing the intracellular levels of reactive oxygen species (ROS) and modulating some redox-sensitive proteins and survival pathways.[19−21] Therefore, curcumin has the potential for the treatment of AD. In clinical trial, in respect to AD, it appears to be safe and tolerable with no adverse chronic effect until the high dose of 4 g/day during 6 months.[22] In spite of its *in vitro* and *in vivo* efficacy and its safety, curcumin has not yet been approved as a therapeutic agent due to its poor oral bioavailability caused by the high hydrophobicity of the molecule. Thus, to enhance its solubility and stability, we have encapsulated this compound into biodegradable poly(lactide-*co*-glycolide) (PLGA 65:35) nanoparticles with a ratio of 65% of lactic acid (LA) and 35% of glycolic acid (GA) (NPs-Cur 65:35).[23]

PLGA has been extensively studied for the development of drug carriers and delivery systems.[24] Moreover, it has currently been approved by the Food and Drug Administration (FDA) for human use (see review in ref 25).

We found that NPs-Cur 65:35 displayed suitable delivery properties, for example, small size, high encapsulation efficiency, prolonged release features in our physicochemical conditions, prolonged antioxidant activity, no toxicity, and high neuronal uptake of curcumin with a wide intracellular distribution.[23] More interestingly, curcumin activities were preserved after at least 6 months of storage.[23]

The architecture of nanocarriers not only depends on the nature of compounds to be encapsulated, but also depends on the properties of the polymer and on targeted cells. The ideal matrix should allow low polymeric accumulation and an adequate *in vivo* release profile enabling a minimal drug concentration to be maintained for sustainable effect. Therefore, the choice of a polymeric matrix is indeed of great importance when encapsulating and delivering a drug. For instance, the hydrophilicity is known to influence the kinetic of the degradation of the polymeric matrix. In the case of PLGA, its hydrophilicity decreased when the LA:GA ratio increased. Thus, the kinetic of the PLGA degradation followed this order PLGA 65:35 > 75:25 > 85:15.[26] Another important parameter to consider when formulating nanoparticles is the intrinsic physicochemical nature of the compound to be encapsulated. Previously, we had chosen PLGA 65:35 based on its high entrapment efficiency of curcumin, a highly hydrophobic drug. However, another important parameter to investigate is the ability of the matrix to control the kinetic of the drug release in regard to sink condition and better improve the overall efficiency of our nanosystem. The aim of this study was to get further insight into the property of NPs-Cur to better understand the effect of intrinsic polymer modifications on the activity of entrapped drug. By using PLGA 50:50, we found that NPs-Cur also preserved and enhanced the neuroprotective activity of curcumin by modulating survival networks such as NF-κB, Nrf2, and synaptic activity with Akt and Tau phosphorylation, all of which are implicated in the pathogenesis of AD. Moreover, we found that NPs-Cur can upregulate the expression of some stress-related genes affected during neurodegenerative diseases such as apolipoprotein E (*APOE*), apolipoprotein J (*APOJ*), thioredoxine (*TRX*), glutaredoxine (*GLRX*), and Repressor Element-1/Neuron-Restrictive Silencing Element (*RE-1/NRSE*) REST. We found that NPs-Cur 50:50 were better than free curcumin and NPs-Cur 65:35 in counteracting the increase of *REST* and *GLX* expressions.

Overall, these results provide a new insight into the neuroprotective activity of NPs-Cur and its development as an effective nanomedicine strategy for the treatment of AD. This confirms and opens a new insight in the development of more sophisticated formulations, such as ligands decorated nanocarriers for the active targeting of the brain.

MATERIALS AND METHODS

Materials. Curcumin, PLGA 50:50 (MW = 30−60 kDa) and 65:35 (MW = 40−60 kDa), dimethylammonium bromide (DMAB), dialysis bag (12 kDa), bovine serum albumin (BSA), hydrogen peroxide (H_2O_2), minimal essential medium Eagle (MEM), fetal bovine serum (FBS), penicillin, streptomycin, sodium pyruvate, and antirabbit were obtained from Sigma-Aldrich (Oakville, ON, Canada). PLGA (50:50) nanoparticles loaded with 1 wt % of the fluorescent dye Lumogen Red (NPs-Lumogen) were prepared as described previously[27] and stabilized by 0.1 mg/mL of BSA. Ethyl acetate was purchased from Fisher (Ottawa, ON, Canada). 2′,7′- Dichlorofluorescein-diacetate (DCFDA) was from Invitrogen (Burlington, ON, Canada). Nuclear protein extraction kit was from Active Motif (California, USA). The bicinchoninic acid (BCA) protein estimation kit was from Pierce Biotechnology (Rockford, USA). All chemicals were of analytical grade and used without further purification. Milli-Q water was used for all the experiments. Rabbit polyclonal antiphospho-Akt (pAkt-Ser473) was purchased from Cell Signaling Technology. Polyclonal rabbit polyclonal Keap 1 and anti-Nrf2 antibodies were from Abcam (Cambridge, MA, USA). Rabbit polyclonal anti-NFκB p50 antibody was from Delta Biolabs (Gilroy, CA, USA). Rabbit polyclonal anti-pTau (ser 214) antibody was from Santa Cruz Biotechnology (Dallas, Texas, USA). Mouse monoclonal anti-GAPDH antibody was from Chemicon (Millipore, Mississauga, ON, Canada). Rabbit and mice horseradish peroxydase (HRP) were obtained from Sigma-Aldrich, Inc. Fluorescence emission with different probes was recorded using Synergy HT Multi-Detection Microplate Reader.

Methods. *Preparation of NPs and NPs-Cur.* NPs-Cur formulations were prepared by an emulsion-diffusion-evaporation method, as previously reported.[23] Briefly, curcumin and polymer were dissolved in ethyl acetate (9 mL). Then this organic phase was added to an aqueous phase (17.5 mL) containing DMAB stabilizer (1% w/v) to form an emulsion. This emulsion was stirred and homogenized (Polytron PT4000; Polytron Kinematica, Switzerlandchange) to reduce droplet size. Then the emulsion was further diluted with ultrapure water (132 mL) for solvent diffusion and then subsequently evaporated to remove the organic phase under reduced pressure. NPs-Cur were prepared at a 15% (curcumin/polymer) weight ratio. For the formulation of blank NPs, the same procedure was followed without curcumin.

Nanoparticles were thereafter purified by three cycles of centrifugation (20 000*g*)/resuspension in ultrapure water.

DOI: 10.1021/acs.molpharmaceut.5b00611
Mol. Pharmaceutics 2016, 13, 391−403

Physicochemical Characterization of Nanoformulations. Particle Size and Zeta Potential. Dynamic light scattering (DLS) was used for the measurement of average hydrodynamic diameters and the polydispersity index (PDI) of NPs and NPs-Cur. Measurements were performed using a Zetasizer from Malvern Zetasizer Nano-ZS, Malvern Instruments, UK. Effective mean diameter of the nanoparticles was obtained from three runs for three different samples. Zeta potential data were measured through electrophoretic light scattering (ELS, 20 °C, 150 V) in triplicate for each sample (Malvern Zetasizer Nano-ZS, Malvern Instruments, UK). For both DLS and ELS measurements, water was taken as the dispersant medium.

Transmission Electron Microscopy (TEM). The morphology and the size of NPs and NPs-Cur were observed using TEM (Hitachi H-7100) at 40 000× magnification. Briefly, a drop (100 μL) of NPs or NPs-Cur was placed on a copper grid and air-dried. The grid was then immerged in water, air-dried, and then stained by adding one drop of 3% (w/v) phosphotungstic acid (PTA). Then the grid was air-dried before loading in the microscope and photographed.

Entrapment and Drug Loading Efficiency of NPs-Cur. The percentage of drug incorporated during NPs-Cur preparation was determined using a UV−vis spectrophotometer at the wavelength of 420 nm. After centrifugation of NPs-Cur resuspended with acetonitrile, analyses were performed on supernatants. The efficiencies were calculated using the following equations:

$$\text{Entrapment Efficiency (\%)} = (\text{Weight of drug into nanoparticles} / \text{initial weight of drug}) \times 100$$

$$\text{Drug Loading Efficiency (\%)} = (\text{Weight of drug into nanoparticles} / \text{Weight of produced formulation}) \times 100$$

Mean values were reported from three individual experiments.

In Vitro Release Studies. For *in vitro* release study, purified NPs-Cur were freely dispersed in sodium phosphate buffer (pH 7.4, 30 mL). The release medium was supplemented with 3% w/v BSA as a natural solubility enhancer to maintain sink conditions for the lipophilic curcumin.[28] All samples were kept at 37 °C under magnetic stirring and away from light. At various predetermined end points, 1 mL aliquots were collected and centrifuged immediately (20 000*g* for 30 min at 4 °C) to quantify the exact amount of curcumin in the supernatant at each time. The samples were then analyzed by using a UV−vis spectrophotometer at the wavelength of 436 nm in the presence of BSA, which induces a shift of the absorbance from 420−436 nm.[29] The concentration of curcumin released from the NPs-Cur was expressed as a percentage of the total curcumin loaded into the NPs-Cur and was plotted as a function of time.

Antioxidant Activity Assays. 2,2-Diphenyl-1-picrylhydrazyl (DPPH) Radical Scavenging Activities. The DPPH scavenging activity of free curcumin, NPs, and NPs-Cur was measured by a colorimetric method.[30] Twenty microliters of samples (0.5 μM) were mixed with 200 μL of DPPH solution (0.2 mM in 80% ethanol). The reaction mixture was incubated for 30 min in the darkness at room temperature. The absorbance of the resulting solution was measured at 517 nm. A solution containing 80% ethanol was used as a control. The radical scavenging capacity of the tested samples was measured using the following equation: Radical scavenging activity (%) = $[(A_{control} - A_{sample})/A_{control}] \times 100$. Assays were carried out at least in triplicate, and at least three independent experiments were performed.

Oxygen Radical Absorbance Capacity (ORAC) Assay. ORAC assay was conducted using fluorescein as a fluorescent probe according to previous reports[31,32] with slight modifications. Twenty-five microliters of antioxidant [Trolox (1−8 μM) or sample (Cur, NPs and NPs-cur at 0.5 μM)] was mixed with 150 μL of fluorescein and incubated at 37 °C for 15 min. Then 25 μL of AAPH was added to the mixture. The whole assay lasted for 90 min. The fluorescence was determined with the excitation/emission filters at 485/535 nm using a Synergy HT multidetection microplate reader. Trolox and 2,2′-azobis (2-amidinopropane) dihydrochloride (AAPH) solutions were freshly prepared, and fluorescein was diluted from a stock solution (1.17 mM) in 75 mM phosphate buffer. Final ORAC values were expressed as μmol of trolox equivalent /μmol of curcumim. Assays were carried out in triplicate for a minimum of three independent experiments.

Culture Assay. Cell Line. SK-N-SH cells, a human neuroblastoma cell line from ATCC (Manassas, VA, USA), were maintained in EMEM, supplemented with 10% (v/v) FBS, 1% penicillin/streptomycin, and sodium pyruvate (1 mM) in a humidified incubator at 37 °C with 5% CO_2. Cells were grown to 80% confluence and then seeded into multiwell cell culture plates for the experimental procedures.

Intracellular ROS. Intracellular ROS accumulation was measured by following the oxidation of 2′,7 dichlorofluoresceindiacetate (DCF-DA). Briefly, SK-N-SH cells (2×10^4 cells/well) were plated into 96-well plates and allowed to attach for 24 h. After 24 h, cells were starved and cotreated with free curcumin, NPs, or NPs-Cur and 1.0 mM of H_2O_2 for 1 h. DCFDA was added to a final concentration of 10 μM for 20 min. The fluorescence was then determined with the excitation/emission filters at 485/535 nm using a Synergy HT multidetection microplate reader.

Curcumin Uptake in SK-N-SH Cells by Fluorescence Microscopy. Curcumin is naturally fluorescent in the visible green spectrum. To study the qualitative cellular uptake of the NPs-Cur, SK-N-SH cells were cultured on coverslips coated with poly-D-lysine at a density of 1.5×10^4 cells/well in 24-well plates. Cells were incubated for 24 h at 37 °C and then treated with 0.5 μM free curcumin (used as positive control) or NPs-Cur for 1 h. Cells were then fixed with methanol and the nuclei stained with 1 μg/mL of DAPI for 15 min.

In another experiment, cells were incubated with fluorescent polymer nanoparticles, NPs-Lumogen, for 4 h at 37 °C. The glass slides were mounted with prolong gold antifade reagent, protected from light, and air-dried. For fluorescence microscopy (Leica ECB, Germany), images were captured using a camera (SensiCam high performance) under the DAPI filter for DAPI detection and the FITC filter for curcumin signal detection. The mean of the intensity of fluorescence per surface unit in each condition was then quantified using the Image-Pro plus 5.0 software (Media Cybernetics, USA), and Log2 change over nontreated cells was calculated.

Protein Extraction. SK-N-SH cells were treated with 1 mM H_2O_2 and 0.5 μM free curcumin, NPs, or NPs-Cur for 30 min (Nrf2 and P50) or for 1 h (pAkt, pTau, and Keap1). Total proteins of SK-N-SH cells were extracted with a lysis buffer containing a cocktail of protease inhibitors, and nuclear

DOI: 10.1021/acs.molpharmaceut.5b00611
Mol. Pharmaceutics 2016, 13, 391−403

proteins were extracted using a kit from Active Motif. Total and nuclear proteins were quantified using the BCA test.

Western Blot Analysis. Equal amounts of protein cell lysates (30 μg) were separated on 10% sodium dodecyl sulfate polyacrylamide gel electrophoresis (SDS-PAGE) gels and transferred into PVDF membranes. Membranes were blocked for 1 h in TBS with 5% skim milk and incubated with primary antibodies: anti-Keap 1 (1/700), pAkt (1/1000), anti-Nrf2 (1/1000), anti-NF-κB p50 (1/500), anti-pTau (1/500), and anti-GAPDH (1/1000). Amido black 1X was used for rapid staining of total protein bands. Blots are stained for 1 min and then destained for 30 min in 25% (v/v) isopropanol, acetic acid 10% (v/v). Then membrane was incubated with the secondary antibody HRP-conjugated antirabbit or antimouse (1/10 000) for 1 h. Detection was realized with Immobilion Western Chemiluminescent HRP Substrate, and the bands were visualized and quantified by densitometric analysis using luminescent imaging system FluorChem.

Gelatin Zymography. SK-N-SH cells were cotreated with 0.5 μM curcumin, NPs, or NPs-Cur and with 1 mM H_2O_2 for 1 h. The supernatants (30 μL corresponding to 1×10^6 cells) were mixed with a 4× nonreducing LaemmLi's sample buffer (40% glycerol, Tris-HCl 1 M pH 6.8, SDS 8%) and run on 7.5% acrylamide gels containing 2 mg/mL of gelatin. Gels were washed for 30 min twice with 2.5% Triton X-100 and incubated overnight in digestion buffer (Tris-HCl 50 mM pH 7.4, NaCl 150 mM and $CaCl_2$ 5 mM). Gels were stained with Coomassie blue 0.1% and destained.

Gene Expression Analysis by Real-Time PCR (qRT-PCR). Expression of APOE, APOJ, TRX, GLRX, and REST genes by human SK-N-SH neuroblastoma cells was assessed. TRIzol Reagent (Invitrogen, La Jolla, CA) was used to extract total RNA from 1.5×10^6 cells unexposed or exposed to 500 μM H_2O_2 for 4 h. Cells were cotreated with (curcumin, NPs, or NPs-Cur). After extraction, RNA purity and degradation were checked by spectrophotometry using BioSpecnano (Shimadzu Corporation, Kyoto, Japan) and capillary electrophoresis using RNA 6000 Nanokit and the Bioanalyzer2100 (Agilent Technologies, Santa Clara, CA). The complementary DNA (cDNA) synthesis was performed with 100 ng of total RNA using the iScriptcDNA synthesis Kit (Bio-Rad, Marnes-la Coquette, France) following the manufacturer's protocol. Gene expressions were determined by qRT-PCR with the iQ SYBR Green Supermix (Bio-Rad) in a Stratagene Mx3000p system (Agilent Technologies).

Briefly, 4 μL of each cDNA sample was amplified in a PCR reaction (final volume of 20 μL) containing 10 μL of PCR reagent and 300 nM of each of the two primers (Table 1). For all samples, the following conditions were used: an initial heat-denaturing step at 95 °C for 5 min followed by 40 cycles of 95 °C for 15 s, annealing at 60 °C for 40 s, and elongation and signal acquisition at 72 °C for 40 s. To confirm the amplification of specific transcripts, melting curve profiles were produced at the end of each reaction, and if two or more peaks were present, the corresponding results were excluded. Water was used as negative control for each PCR run. For each gene, amplifications were performed from three independently prepared samples. Gene expression levels were normalized by comparison to beta-actin (ACTB), used as reference gene. Fold change (FC) of gene expression was calculated by $2^{-\Delta\Delta Ct}$ method.[33]

Statistical Analysis. All data were expressed as means ± SEM from at least three independent experiments performed at least in triplicate. Statistical analysis was performed by a Dunnett's test. For Western-blot analysis, one-way ANOVA followed by Tukey test were used. The level of significance was considered when $p < 0.05$.

Table 1. Primers Used for Gene Expression Analysis

genes	primers
ApoE	F: 5′−GGT-CGC-TTT-TGG-GAT-TAC-CT−3′
	R: 5′−TCC-AGT-TCC-GAT-TTG-TAG-GC−3′
ApoJ	F: 5′−ACA-ATG-AGC-TCC-AGG-AAA-TG−3′
	R: 5′−TCA-GGC-AGG-GCT-TAC-ACT-CT−3′
GLRX	F: 5′−TCA-GTC-AAT-TGC−CCA-TCA-AA−3′
	R: 5′−GCA-GAG-CTC-CAA-TCT-GCT-TT−3′
TRX	F: 5′−CAG-ATC-GAG-AGC-AAG-ACT-GC−3′
	R: 5′−TTG-GCT-CCA-GAA-AAT-TCA-CC−3′
REST	F: 5′−TGC-GTA-CTC-ATT-CAG-GTG-AG−3′
	R: 5′−CGT-GGG-TTC-ACA-TGT-AGC-TCT−3′
ACTB	F: 5′−TTG-GCA-ATG-AGC-GGT-TCC−3′
	R: 5′−GTA-CTT-GCG-CTC-AGG-AGG-AG−3′

RESULTS

Characterization of NPs 50:50 and NPs-Cur 50:50. Figure 1, panels A and B show that the mean particle sizes, as determined by DLS, were 131 ± 11 nm and 101 ± 4 nm for NPs 50:50 and NPs-Cur 50:50, respectively (Figure 1C,D). TEM was used to confirm the nanoparticles size and determine the spherical morphology of both nanoparticles. The morphology of NPs 50:50 and NPs-cur 50:50 did not differ from that of NPs 65:35 and NPs-Cur 65:35. A smaller size was observed by TEM than by DLS due to the state of the polymeric matrices, which were hydrated in the case of DLS (hydrodynamic diameters) and dried in the case of TEM. Samples prepared from PLGA 65:35 were more polydisperse than those obtained from PLGA 50:50 (Table 2). Zeta potential values were all positive, irrespective of the drug loading in opposite to what is generally observed with PLGA matrices. This phenomenon was linked to the residual tensioactive at the NP surface and was exacerbated when drug was actually present in the formulation (Table 2). This also suggests that a portion of the drug was associated with the NP surface. The amount of drug loading in the nanoparticles plays an important role with respect to the rate and duration of drug release as well as its efficacy. The initial drug loading represents 15% (15 mg of curcumim/100 mg polymer) for both formulations. The entrapment efficiency of curcumin in Nps-Cur 50:50 was determined to be 27 ± 2%, which is lower than Nps-Cur obtained from PLGA 65:35, which was 31 ± 6%. Similarly, the final drug loading efficiency tended to be lower with PLGA 50:50 (5.1 ± 2) than with PLGA 65:35 (6.9 ± 3).

Release Kinetics of Curcumin from NPs-Cur. The *in vitro* release profiles of curcumin from NPs-Cur 50:50 and NPs-Cur 65:35 were studied in phosphate buffer containing 3% BSA at pH 7.4 (Figure 2A). For both formulations, a moderate burst release was noted for the first 5 h, followed by a slower release over 24 h. The release of curcumin from NPs-Cur 65:35 was lower than from NPs-Cur 50:50 reaching 20% and 27%, respectively, after 24 h (Figure 2A).

NPs-Cur Uptake by SK-N-SH Cells. To compare the uptake of curcumin, NPs-Cur 50:50, and NPs-Cur 65:35 by cultured neurons, SK-N-SH cells were incubated with 0.5 μM of free curcumin (control), NPs-Cur 50:50, or NPs-Cur 65:35 for 1 h at 37 °C. Control cells did not display any significant

DOI: 10.1021/acs.molpharmaceut.5b00611
Mol. Pharmaceutics 2016, 13, 391−403

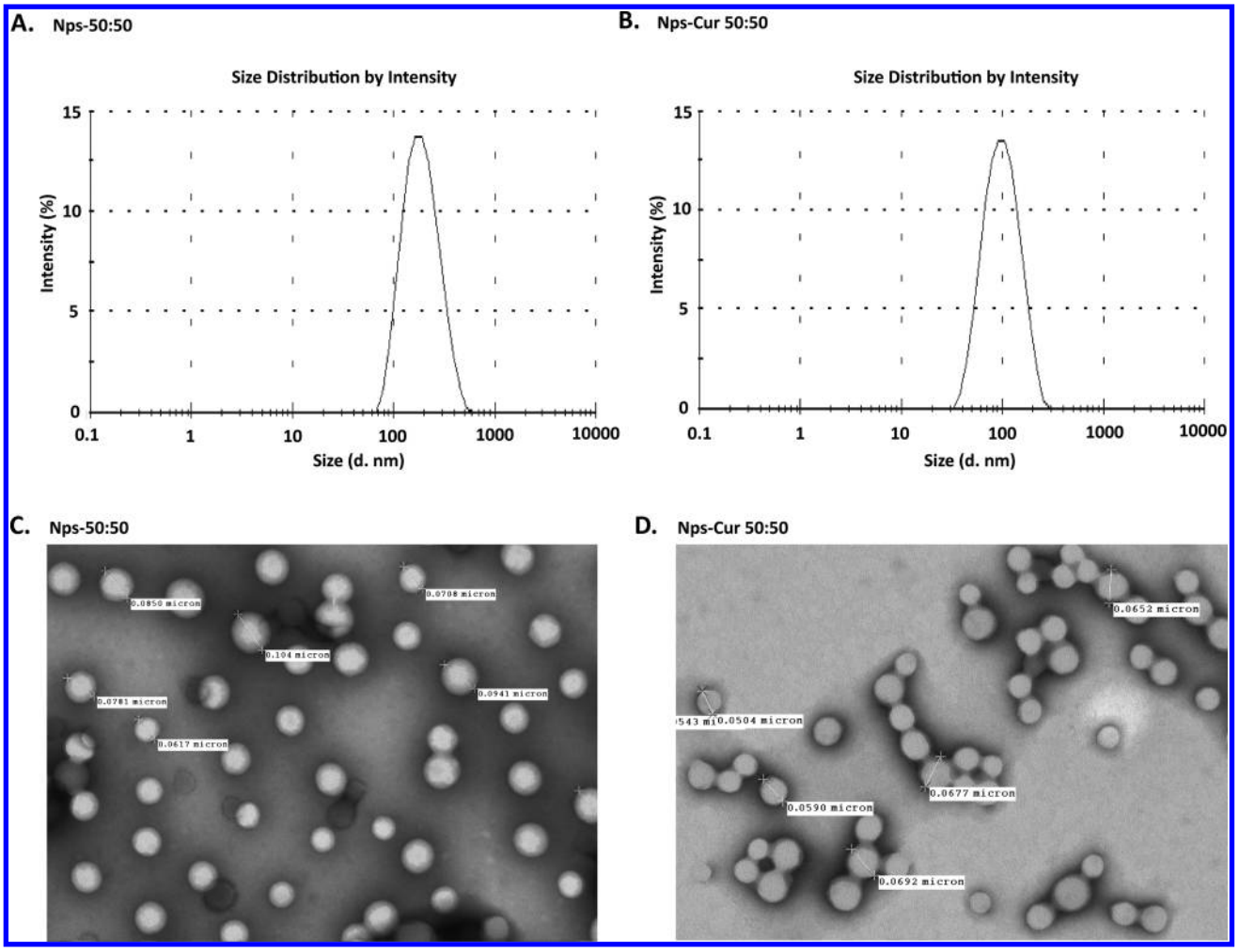

Figure 1. Size distribution and morphological characterization of NPs 50:50 and NPs-Cur 50:50 using dynamic laser light scattering (DLS) and transmission electron micrograph (TEM). DLS analysis of polymeric NPs 50:50 (A) and NPs-Cur 50:50 (B) and TEM photographs of NPs 50:50 (C) and NPs-Cur 50:50 (D).

Table 2. Data on the Particle Size, Drug-to-Polymer Weight Ratio, Entrapment Efficacy, Drug Loading Efficiency, PDI, and Zeta Potential for NPs 50:50, NPs-Cur 50:50, NPs 65:35, and NPs-Cur 65:35 Analyzed by DLS

formulation (n = 3 batches per tested condition)	drug-to-polymer weight ratio (%)	entrapment efficiency (%)	drug loading efficiency (%)	size (d nm)	polydispersity index	zeta potential (mV)
Nps 50:50				131 ± 11	0.30 ± 0.01	6.4 ± 0.3
Nps-Cur 50:50	15	27 ± 2	5.1 ± 2	101 ± 4	0.12 ± 0.03	54.0 ± 2.9
Nps 65:35				148 ± 14	0.25 ± 0.02	16.0 ± 8.2
Nps-Cur 65:35	15	31 ± 6	6.9 ± 3	131 ± 7	0.27 ± 0.02	57.0 ± 3.0

fluorescence, while in the presence of NPs-Cur formulations, cells displayed a clear green fluorescence due to the rapid internalization and accumulation of curcumin inside the cells (Figure 2D,E). The internalization of NPs-Cur formulations was seen primarily in the cytoplasm surrounding the nucleus (Figure 2D,E). Quantitative analysis indicated that the uptake of NPs-Cur 50:50 by SK-N-SH cells was higher than with NPs-Cur 65:35 or free curcumin (Figure 2H). The intracellular green fluorescence corresponds to the fluorescence of curcumin, but it is not clear whether the matrix PLGA is taken up by neuronal cells or not. To analyze whether the PLGA nanoparticles were taken up by neuronal cells, we used PLGA 50:50 NPs loaded with 1 wt % Lumogen Red (NPs-Lumogen). These nanoparticles were demonstrated to be photostable, 10-fold brighter than quantum dots, stable in cell culture media, and are taken up by HeLa cells via endocytosis process without any cytotoxicity.[27] For this purpose, SK-N-SH cells were incubated with NPs-Lumogen for 4 h, and the fluorescence intensity corresponding to the localization of NPs-Lumogen was assessed with the Rhodamine filter (in red). Figure 2, panel F shows the red fluorescence in the vicinity of the nucleus; some fluorescence was observed in the nucleus, but it cannot be excluded that it comes from regions above or below the nucleus. Fluorescence was also observed in the dendrites. Furthermore, the red signal was concentration-dependent, the intensity with 0.3 nM NPs-Lumogen being higher than with 0.2 nM (Figure 2F,G). These results demonstrated that the PLGA NPs could be taken up by neuronal cells and supported the hypothesis that NPs-Cur

DOI: 10.1021/acs.molpharmaceut.5b00611
Mol. Pharmaceutics 2016, 13, 391−403

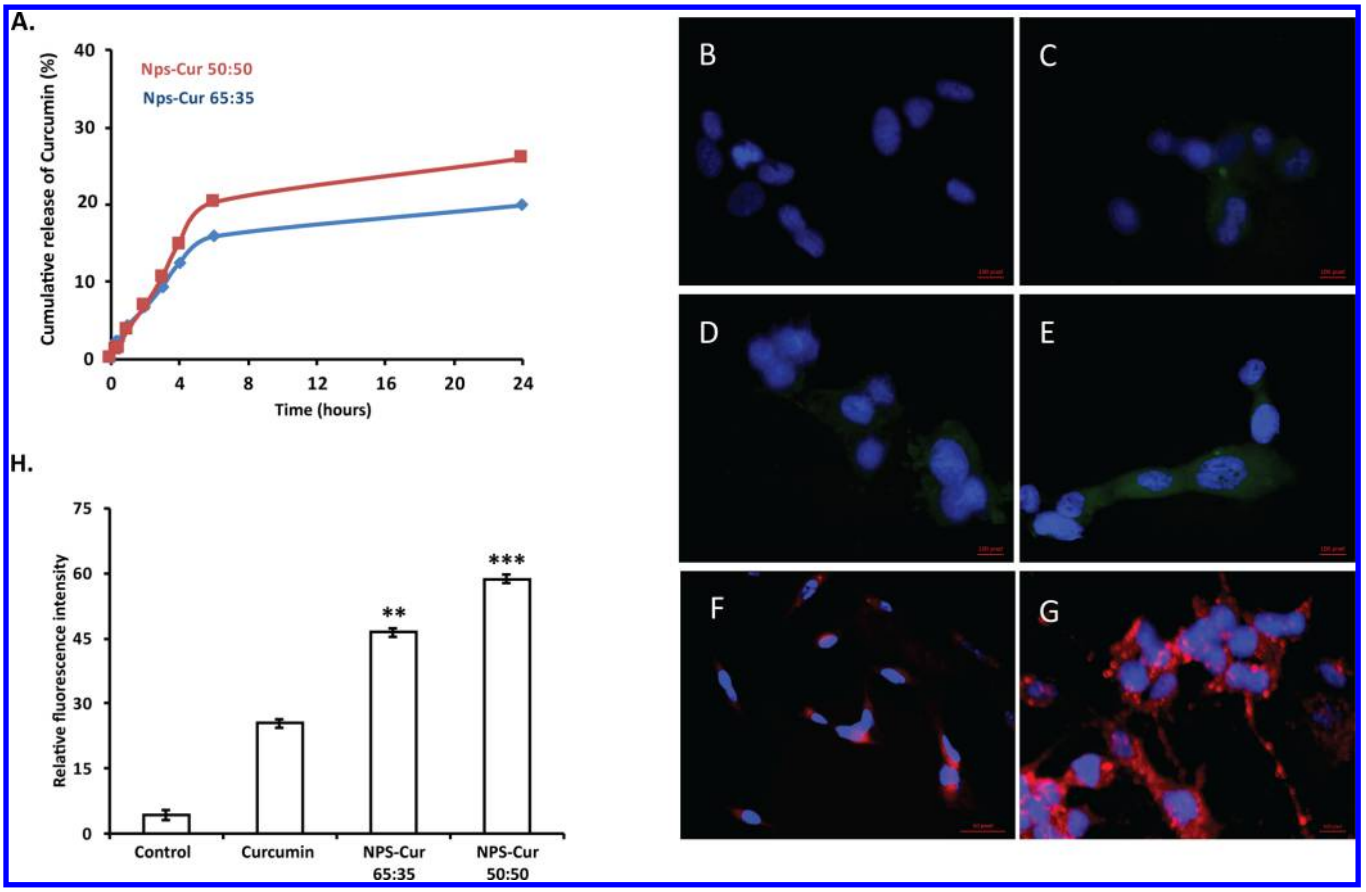

Figure 2. Comparison of *in vitro* release kinetics of curcumin from NPs-Cur 65:35 and NPs-Cur 50:50 in phosphate buffer (pH 7.4, BSA 3%) (A). Fluorescence microscopy imaging of curcumin uptake by SK-N-SH cells. SK-N-SH cells were treated for 1 h at 37 °C with PBS (control, B), free curcumin (C), NPs-Cur 65:35 (D), and NPs-Cur 50:50 (E). Fluorescence of curcumin is observed in green. Lumogen loaded NPs (PLGA 50:50), NPs-Lumogen were used to specify if PLGA nanoparticles are taken up by cells. NPs-Lumogen uptake using fluorescence microscopy is observed in red after an exposure period of 4 h. PLGA internalization is concentration-dependent as observed in panels F and G with, respectively, 0.2 and 0.3 nM of Lumogen. Quantification of the green fluorescence (H) with data representing mean ± SEM from at least three independent experiments with **, $p \leq 0.01$ and ***, $p \leq 0.001$ indicating a statistical difference versus curcumin treated group.

formulations were effectively taken up by neuronal cells with higher cellular uptake than free curcumin.

Antioxidant Activity of the NPs-Cur 50:50 and Their Effects on the Nrf2 Pathway. The DPPH test was assessed to study the free-radical scavenging capacity of NPs-Cur 50:50 in comparison to free curcumin. Blank NPs 50:50 did not show any free-radical scavenging activity, while free curcumin and NPs-Cur 50:50, at 0.5 μM, displayed the same antioxidant capacity (25% of DPPH inhibition) (Figure 3A). This property was then confirmed by the ORAC assay, which measures the antioxidant scavenging activity against the peroxyl radical produced after the thermolysis of AAPH at 37 °C.[36] As shown in Figure 3, panel B, 0.5 μM NPs-Cur 50:50 displayed 1.5- and 2.2-fold higher antioxidant capacity against peroxyl radical than free curcumin and blank NPs, respectively.

The antioxidant effect of NPs-Cur 50:50 was then determined on SK-N-SH cells by DCFDA assay. For that purpose, SK-N-SH cells were treated with curcumin or NPs-Cur 50:50 at three different concentrations (0.07 μM, 0.25 μM, and 0.5 μM) and equivalent concentrations of NPs 50:50. After 1 h of treatment, the intensity of the fluorescence of DCF was significantly reduced for the three different concentrations of free curcumin, NPs-Cur 50:50, and with the highest tested volume of blank NPs 50:50 (Figure 3C). Interestingly, the three tested concentrations significantly reduced the ROS-level induced by H_2O_2 (Figure 3D). These data strengthened the results obtained on DPPH and ORAC assays and demonstrated that curcumin loaded into NPs-Cur 50:50 retained its antioxidant activity. On the basis of the effect of NPs-Cur 50:50 on DPPH, ORAC, and ROS levels, we investigated the effect of NPs-Cur 50:50 on the antioxidant pathway Nrf2/Keap1. To determine the expression level of Nrf2 in the nucleus, SK-N-SH cells were cotreated with 1 mM H_2O_2 for 30 min and with 0.5 μM free curcumin or with an equivalent concentration of NPs-Cur 50:50 or NPs 50:50. In SK-N-SH cells, the activation of Nrf2 by H_2O_2 was prevented in the presence of curcumin, NPs-Cur, and even blank NPs (Figure 4A). Since the activity of Nrf2 is regulated by the inhibitory protein Keap1, we also evaluated the cytoplasmic level of Keap1 in the presence of 1 mM H_2O_2 for 1 h. Accordingly, NPs-Cur 50:50 as well as curcumin also prevented the elevation of the expression of Keap1 induced by H_2O_2 (Figure 4B).

Effects of Free Curcumin, NPs 50:50, and NPs-Cur 50:50 on Inflammatory Pathways. MMP-9 is the major MMP expressed and released by neurons. It contributes to neuroinflammation response in AD.[37] We have thus analyzed the effect of free curcumin at 0.5 μM, NPs-Cur 50:50 at 0.5 μM, and NPs 50:50 with equivalent quantities of curcumin on the levels of gelatinolytic MMPs induced by H_2O_2 in SK-N-SH cells (Figure 5A).

DOI: 10.1021/acs.molpharmaceut.5b00611
Mol. Pharmaceutics 2016, 13, 391−403

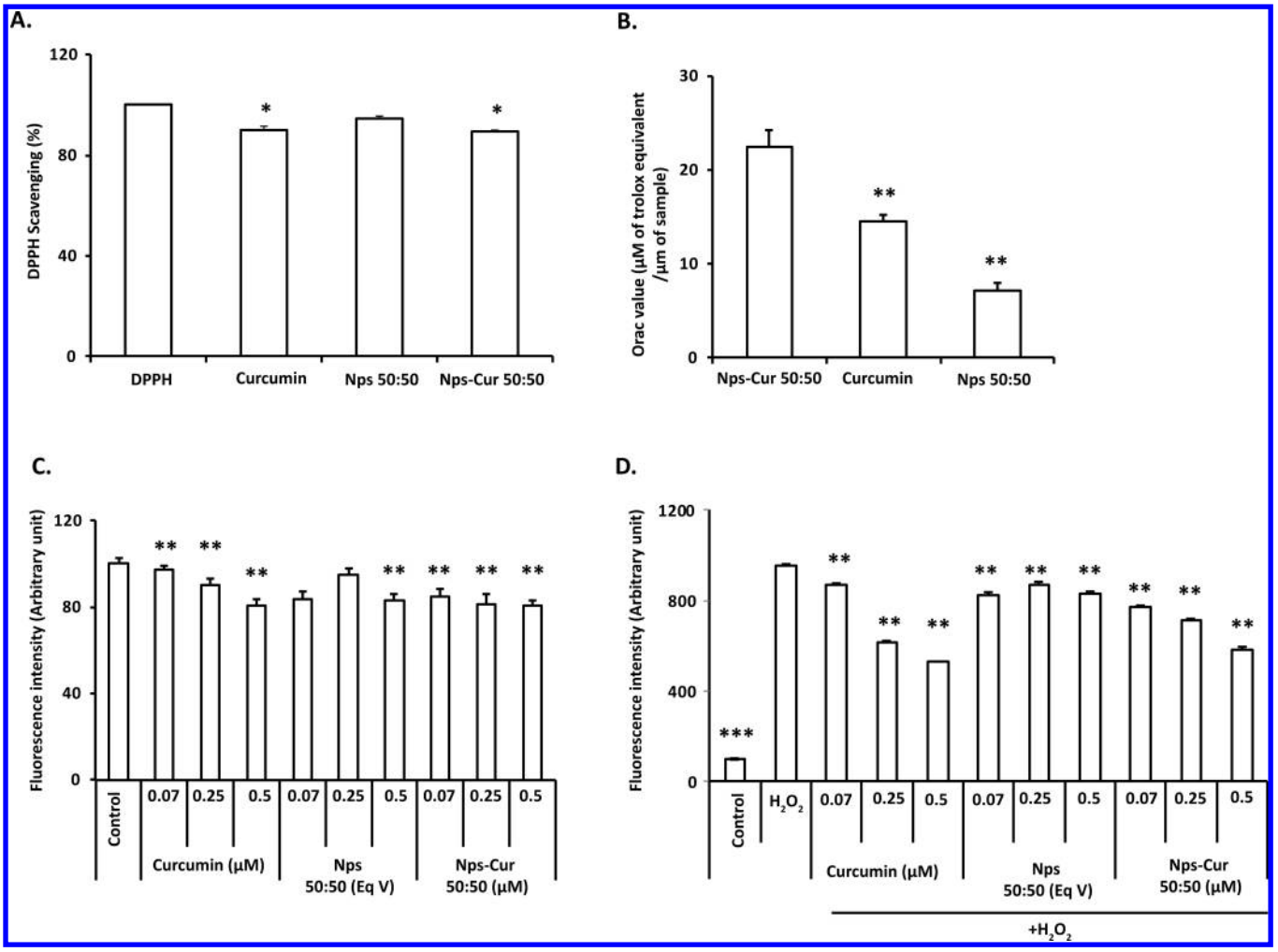

Figure 3. Antioxidant capacity of free curcumin, NPs 50:50, and NPs-Cur 50:50. DPPH radical scavenging activity of 0.5 μM of free curcumin or an equivalent volume of NPs-Cur 50:50 or NPs 50:50 (A); ORAC value performed in the presence of 0.5 μM of free curcumin or an equivalent volume of NPs-Cur 50:50 or NPs 50:50 (B); intensity of DCF-DA analyzed 1h after the treatment of SK-N-SH cells with PBS, different concentrations of free curcumin (0.07 μM, 0.25 μM, and 0.5 μM), or an equivalent volume of NPs-Cur 50:50 or NPs 50:50 in the absence (C) or in the presence of 1 mM of H_2O_2 (D). Results are expressed as percentage of control (considered as 100%). Data represent mean ± SEM from at least three separate experiments performed in triplicate with *, $p < 0.05$ and **, $p < 0.01$ indicating a statistical difference versus control.

Gelatin zymography of the culture media of SK-N-SH cells showed that the release of MMP-9 was inhibited by NPs-Cur 50:50, whereas no effect of curcumin or blank NPs 50:50 was observed. Hence, these results demonstrated that NPs-Cur 50:50 were more efficient than curcumin on MMP-9 activity. We have thus investigated the effect of NPs-Cur 50:50 on the NF-κB pathway by analyzing the cytoplasmic and nuclear expression of the subunit p50 subunit of NF-κB (Figure 5B,C). For this, SK-N-SH cells were cotreated for 30 min with 1 mM H_2O_2 and with 0.5 μM of curcumin or NPs-Cur 50:50 or with an equivalent concentration of NPs 50:50. Curcumin and NPs-Cur reduced the level of the subunit p50 in the cytoplasm and its nuclear translocation induced by H_2O_2.

Effects of Free Curcumin, NPs, and NPs-Cur on pAkt/pTau Pathways. To determine whether Akt pathway is implicated or not in the neuroprotective effect of NPs-Cur, we have examined the phosphorylation of Akt at the serine 473 by Western blot. The results showed that curcumin, NPs 50:50, and NPs-Cur 50:50 decreased Akt phosphorylation induced by H_2O_2 (Figure 6A). Our results also demonstrated that oxidative stress induced the phosphorylation of Tau at the Ser 214. Interestingly, both curcumin and NPs-Cur 50:50 treatments suppressed this phosphorylation (Figure 6B).

Effects of NPs-Cur on Gene Expression Analysis. The effects of PLGA nanoparticles on the expression of key genes involved in neuroprotection and antioxidant pathways have been poorly studied. We have therefore evaluated the effects of PLGA nanoparticles (50:50 and 65:35) on the expression of *GLRX*, *TRX*, *REST*, *APOJ*/*Clusterin*, and *APOE*. Our results showed that these genes were constitutively expressed in SK-N-SH cells and not modified by blank NPs after 4 h of treatment. The effect of H_2O_2 on the expression of some of these genes is well-known. For example, both thioredoxin and glutaradoxin were overexpressed after exposure to H_2O_2 and remained elevated for 24 h.[38] However, in the presence of curcumin or NPs-Cur, we observed an induction of GLRX and TRX levels, a decrease of APOJ mRNA levels, while the levels of APOE and REST remain at the initial control expressions (Figure 7). In the presence of H_2O_2, both NPs-Cur (50:50 and 65:35) were more efficient than free curcumin to prevent the induction of the five analyzed genes (Figure 8).

DOI: 10.1021/acs.molpharmaceut.5b00611
Mol. Pharmaceutics 2016, 13, 391−403

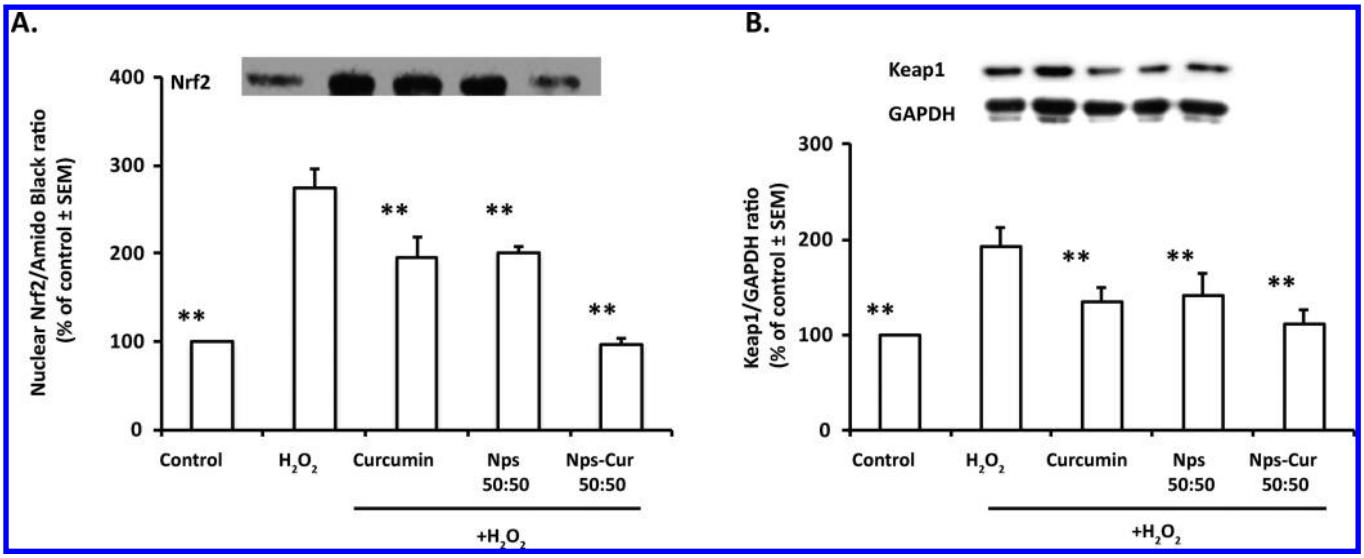

Figure 4. Effects of free curcumin, NPs 50:50, and NPs-Cur 50:50 on the Nrf2 activity. After 1 h of treatment, the level of Keap1 was analyzed on total proteins (A), and Nrf2 levels were also determined on nuclear fraction (B). Blot represents one of the three independent experiments, and bar graph represents quantitative results of the ratio between Keap1 and GAPDH, Nrf2, and amido black. Densitometry analyses were performed on all three experiments, and results are expressed as percentage of control (considered as 100%) with **, $p < 0.1$ versus H_2O_2 treated group.

DISCUSSION

Effective drug delivery to the CNS for the treatment of neurodegenerative diseases such as AD remains a great challenge. Over the past few years, significant breakthroughs have been made in developing suitable PLGA NPs to protect drugs from enzymatic degradation, to increase their bioavailability,[39,40] and eventually for their delivery across the blood–brain barrier (BBB). Curcumin is one of the most extensively investigated natural compounds for the treatment of AD.[18] Previously, we had successfully encapsulated curcumin in polymeric PLGA nanoparticles with a LA/GA ratio of 65:35 (NPs-Cur 65:35).[23]

Nevertheless, the characteristics of the biodegradable polymer strongly impact the degradation and hence the erosion of the matrix. PLGA is a copolymer of D,L-lactic acid (LA) and glycolic acid (GA) with a wide range of LA/GA ratios and molecular weights and therefore can display various physicochemical and degradation properties for controlled drug release applications. Since GA is slightly more hydrophilic than LA, the higher the GA content, the faster the hydrolysis rate. Thus, the LA/GA ratio can modulate the hydophobicity and crystallinity of the system and therefore the erosion of the matrix, the burst release, and the rate of matrix degradation in cells.

To get further insight into the properties of NPs-Cur, in this study, we have investigated the effect of the polymer PLGA 50:50 on the preservation of the neuroprotective and antioxidant activities of curcumin. We found that both PLGA polymers (50:50 and 65:35) led to nanocarriers with an acceptable size distribution and the similar entrapment and drug loading efficiency. In fact, in this study, we found that the size of curcumin-encapsulated PLGA nanoparticles (50:50) was smaller than that of bare PLGA nanoparticles. This phenomenon was previously reported by several studies where hydrophobic drugs are loaded into PLGA 50:50 matrices.[23,34,35] In our point of view, blank PLGA nanoparticles display a higher volume due to their higher hydratation state, while in the presence of encapsulated curcumin, this hydrated state is decreased due to the presence of a more hydrophobic core. Moreover, the strong hydrophobic interactions between the PLGA matrix and curcumin could lead to a more structured nanoparticle core, also resulting in smaller nanoparticles. However, NPs-Cur 65:35 was found to be bigger than 50:50 indicating that the polymer ratio of lactic acid/glycolic acid interferes on this parameter. This latter point can be related to the more numerous microcrystalline domains in the case of the 65:35 matrix, leading to a lower aptitude to chain folding during the NP formation and thus to bigger nancarriers.[25]

In both cases, the zeta potential was lower in blank NPs than in NPs-Cur indicating the presence of curcumin at the NP surface could be implicated in the nanosuspension stability. We found that the release of curcumin entrapped in the PLGA 50:50 matrix was significantly faster than in PLGA 65:35. This phenomenon could be explained by two parameters: (i) the higher affinity of curcumin for the more hydrophobic PLGA 65:35 matrix could reduce the drug release rate; (ii) the more hydrophilic nature of PLGA 50:50 could lead to a faster and more important diffusion of water molecules inside the nanocarrier matrix and therefore lead to a faster drug release. This could also explain why blank NPs were found bigger, for example, more hydrated than NPs-Curc. Taken together, these results suggest that the composition of the polymer influences NPs formation and drug release through hydrophobic interactions and nanocarrier hydratation.

The release kinetics of curcumin was found to be biphasic with a moderated burst effect noted between 0 to 6 h, reaching a maximum release of 15% and 20% for NPs-Cur 50:50 and NPs-Cur 65:35, respectively. This rapid phase corresponds to the surface release of curcumin, as usually observed for this type of PLGA nanocarriers.[23,25] However, because of the hydrophobic nature of curcumin and despite the presence of a solubility enhancer, this phase was lesser in intensity compared to what is observed for more hydrophilic drug compounds.[41] The second slope depicted a quasilinear behavior after 5 h, which may represent a combination of water diffusion and very slow and gradual erosion of PLGA-matrix. Other studies have reported a release of less than 40% curcumin in 24 h with copolymeric micellar aggregates of NIPAAM and VP.[42] The

DOI: 10.1021/acs.molpharmaceut.5b00611
Mol. Pharmaceutics 2016, 13, 391–403

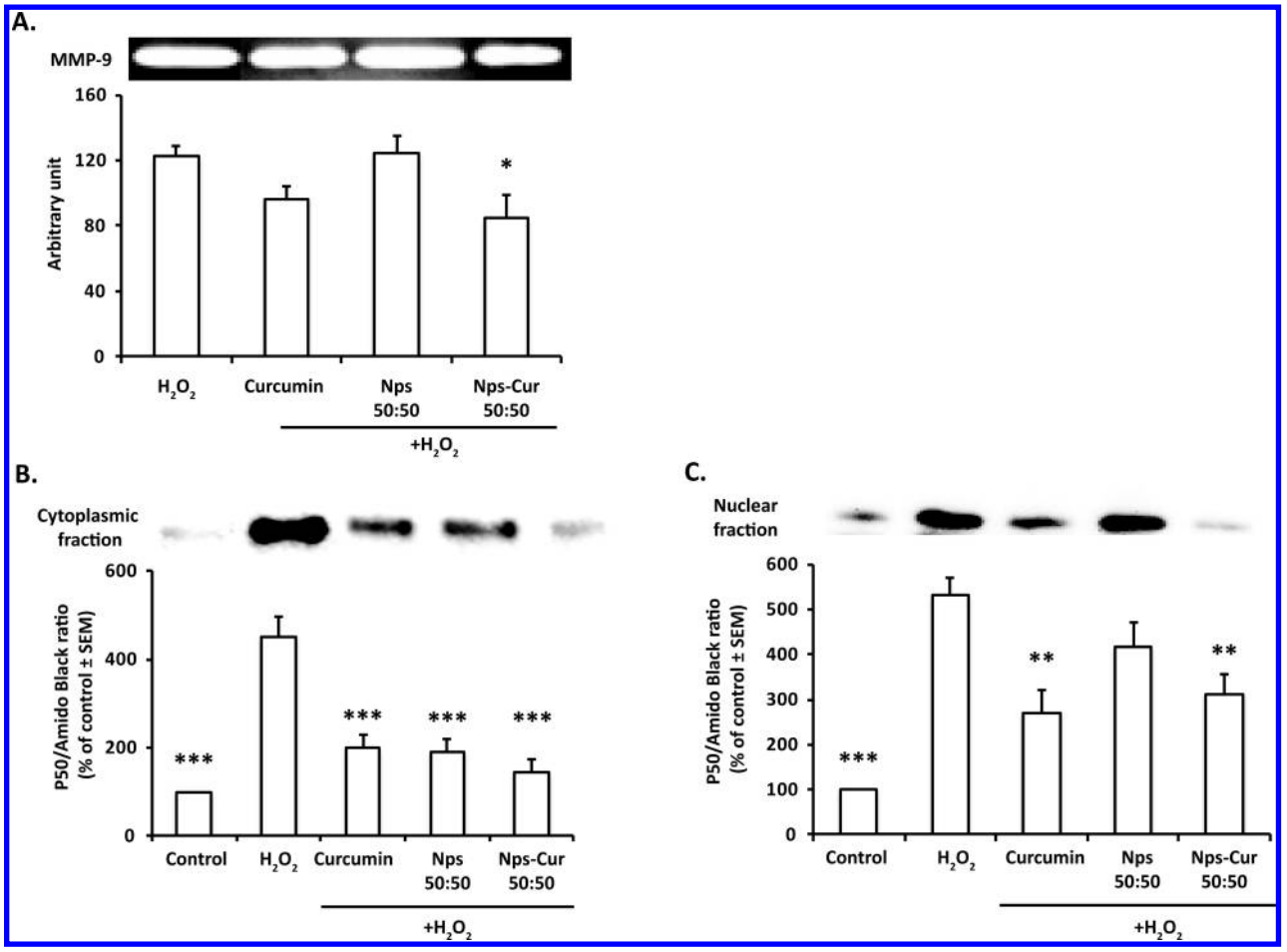

Figure 5. Effects of free curcumin, NPs 50:50, and NPs-Cur 50:50 on the enzymatically active gelatinase induced by H_2O_2. Extracellular release of MMP-9 (gelatinase) was evaluated using gelatin zymography experiments, and densitometry analysis of gelatinase activity is presented (A). Data represent mean ± SEM from at least three separate experiments with ∗, $p < 0.05$ indicating a statistical difference versus H_2O_2. Level of the p50 subunit of NF-κB was also analyzed after 30 min of treatment in the cytoplasmic (B) and nuclear fraction (C). Blot represents one of the three independent experiments, and bar graph represents quantitative results of the ratio with amido black. Densitometry analyses were performed on all three experiments. Results are expressed as percentage of control (considered as 100%) with ∗∗, $p < 0.01$ and ∗∗∗, $p < 0.001$ versus H_2O_2 treated group.

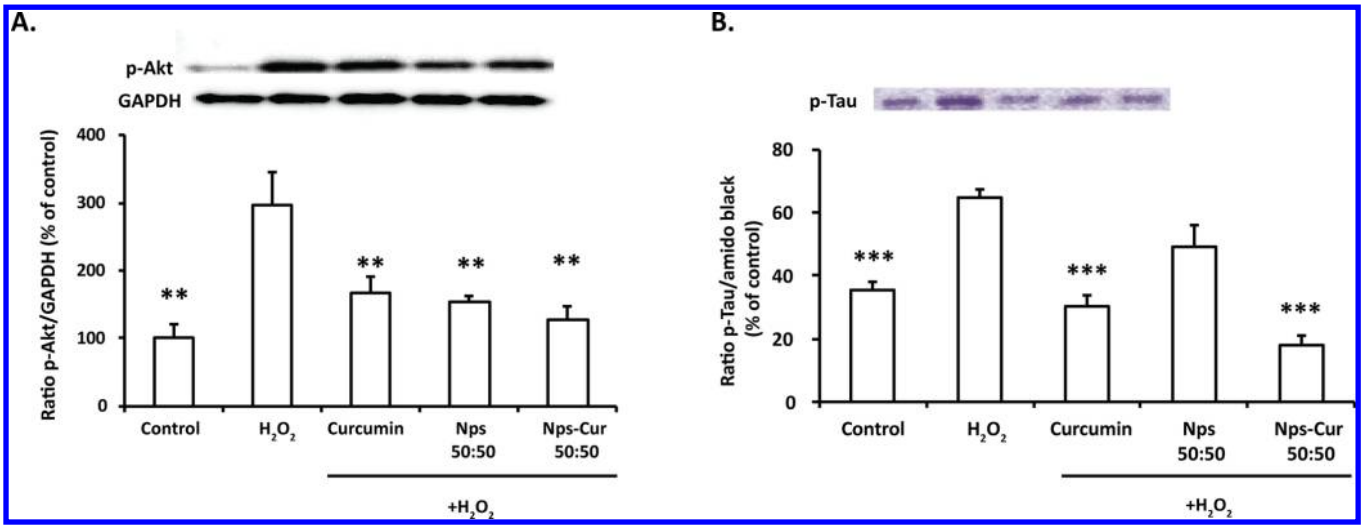

Figure 6. Effects of free curcumin, NPs 50:50, and NPs-Cur 50:50 on Akt and pTau pathways. After 1 h of treatment, the levels of pAkt (A) and pTau (B) were measured on total proteins. Blots represent one of the three independent experiments, and bar graph represents quantitative results of the ratio between pAkt/GAPDH and pTau/amido black. Densitometry analyses were performed on three experiments. Results are expressed as percentage of control (considered as 100%) with ∗∗, $p < 0.01$ and ∗∗∗, $p < 0.001$ indicating a statistical differences versus H_2O_2 treated groups.

DOI: 10.1021/acs.molpharmaceut.5b00611
Mol. Pharmaceutics 2016, 13, 391−403

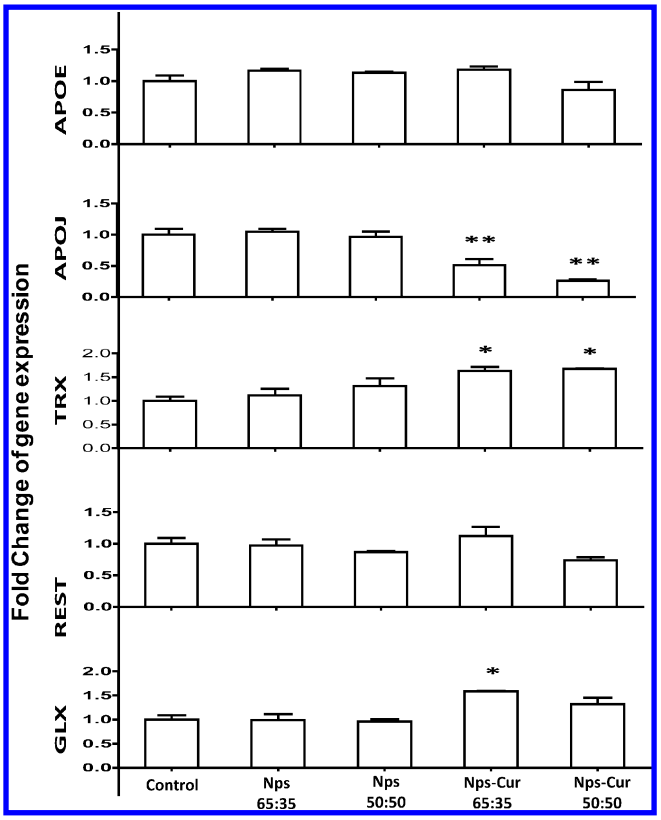

Figure 7. Effect of void nanoparticles on gene expression changes in neuronal cells. SK-N-SH cells were exposed to either PLGA void nanoparticles (50−50 and 65−35) or NPs-Cur. The equivalent volume of formulation required to have 0.5 μM of curcumin for each formulation was used to have the same range of polymer concentration. Results were presented as fold change. Data represent mean ± SEM from at least three separate experiments with ∗, $p < 0.05$ and ∗∗, $p < 0.01$ versus control group.

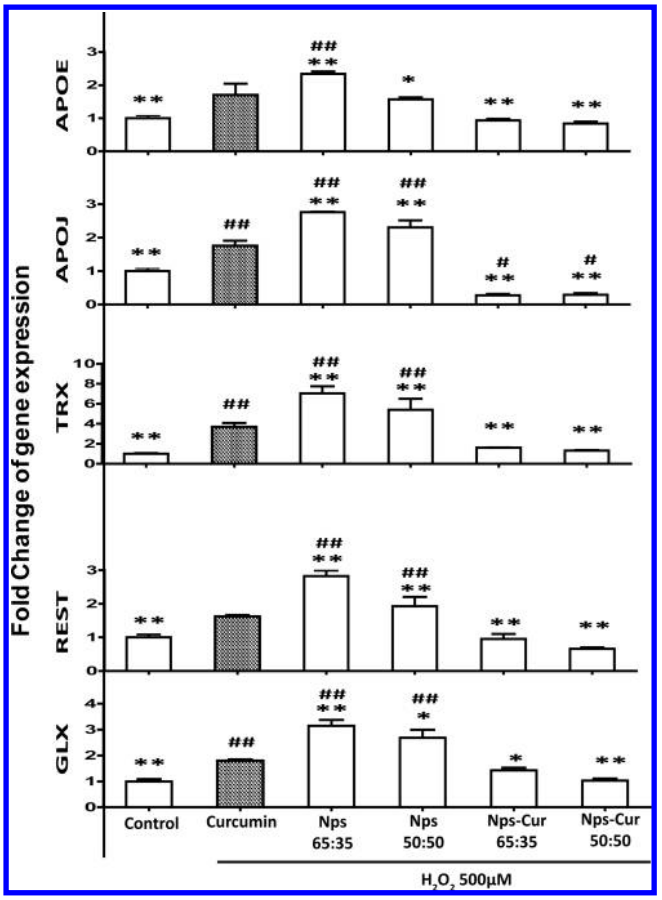

Figure 8. Effect of curcumin encapsulation on gene expression changes in neuronal cells. SK-N-SH cells were exposed to either free curcumin or curcumin loaded NPs (50−50, 65−35) in the presence of 500 μM of H_2O_2. The concentration of curcumin was 0.5 μM for each treatment. Results were presented as fold change with ∗, $p < 0.05$ and ∗∗, $p < 0.01$ versus free curcumin in the presence of H_2O_2, while #, $p < 0.05$ and ##, $p < 0.01$ indicate statistical significant values with respect to control samples.

fact that just 20−25% of drug was released after 24 h was very interesting since more than 70% of curcumin was therefore still available for a sustainable effect. Encapsulation of curcumin not only protected it from rapid degradation, but also enabled its slow and sustained release as evidenced in our subsequent experiments through its biological activities. This enabled the formulation to exhibit a much higher protection found after 24 h through counteracting Akt/Tau hyperphosphorylation, oxidative stress, and expression of some related genes than with free curcumin.

Studying the physical drug release, we have previously demonstrated that curcumin release kinetics fits a Higuchi model using ethanol−water. Here, on a system mimicking the physiological *in vivo* conditions, the difference in the release rate observed between NPs-Cur 50:50 and NPs-Cur 65:35 suggested that polymer composition also represents an important factor in the control of the drug release by the nanoparticles. Indeed, it has recently been demonstrated by Fourier transform infrared (FTIR) and X-ray diffraction (XRD) studies that interactions might occur between the encapsulated curcumin and PLGA polymer matrix by a possible formation of intermolecular hydrogen bonds between the curcumin O−H and PLGA C═O.[43,44]

Our results on DPPH and ORAC assays demonstrated that the antioxidant properties of curcumin are preserved in PLGA NPs-Cur. Moreover, in ORAC assay, NPs-Cur displayed a higher peroxyl radical scavenging activity as compared to free curcumin. It is interesting to note that blank PLGA NPs displayed an antioxidant activity. The recombination between peroxyl free radicals and PLGA chains could reduce ROS level.[45]

To validate the biological activity of NPs-Cur, we have analyzed their effects on three signaling pathways (Nrf2, NF-*k*B, and Akt/pTau) involved in the regulation of oxidative stress, inflammation, neuronal survival, and on the phosphorylation of tau protein, which are all relevant in the pathophysiology of AD.[46] Our results also demonstrated that the property of curcumin on Nrf2 activity is maintained for PLGA 50:50 NPs-Cur and it is similar to PLGA 65:35 NPs-Cur.[23] NF-κB is a well-known transcription factor involved in the regulation of inflammatory responses, which triggers the activity of MMP-9. We found that NPs-Cur 50:50 treatment resulted in reduced expression of MMP-9 with higher efficiency than free curcumin. This can be attributed to the gradual release of curcumin from PLGA nanoparticles and the enhancement of cellular uptake of NPs-Cur. These data are in accordance with the anti-inflammatory activity of curcumin, which is mediated through the inhibition of NF-*k*B.[47] Indeed, these data demonstrated that curcumin encapsulated in PLGA

DOI: 10.1021/acs.molpharmaceut.5b00611
Mol. Pharmaceutics 2016, 13, 391−403

NPs is more potent than free curcumin to inhibit NF-*k*B expression.

Akt is a downstream effector of phosphatidylinositol 3-kinase (PI3−K) signaling pathway. It is directly activated by oxidative stress and is altered in AD brains.[48] We found that Akt phosphorylation induced by H_2O_2 was observed in parallel with tau phosphorylation likely due to the activation of GSK3ß and its dephosphorylation at the serine 9.[49] NPs-Cur 50:50, as curcumin, treatments efficiently prevented Akt activity and Tau phosphorylation. These data demonstrated that NPs-Cur preserve the ability to regulate the Akt/GSK3ß pathway and Tau phosphorylation.[50]

Tiwari et al.[51] have recently demonstrated that PLGA NPs-Cur induced the expression of genes involved in cell proliferation, neuronal differentiation by activating the Wnt/ß-catenin pathway. The effects of NPs-Cur on the expression of genes sensitive to cellular redox remain to be analyzed. Therefore, we have studied the effects of PLGA polymers (50:50 and 65:35) NPs-Cur on the expression of *APOE*, *APOJ*, *TRX*, *GLRX*, and *REST*. These genes are known to be extremely sensitive to ROS.[52] For instance, the sequence of *APOJ* gene contains several putative binding sites for redox-responsive transcription factor including AP1 and Sp1.[53] ApoE displays antioxidant,[54] and ApoE/HDL is well-known to play a crucial role in cholesterol homeostasis in the brain CNS and is involved in neurite outgrowth and synapse formation.[55] The Trx and the Grx systems are among the key components of the thiol redox buffering system, which is essential for maintaining the balance of the cellular redox status. They play an important role in protecting thiol groups from oxidation and to repair those that may have become oxidized. Grx plays important role in glutathionylation/deglutathionylation reactions. Both systems play an important role in neuroprotection and in AD.[56,57] REST was found to potently protect neurons from oxidative stress and is lost in AD.[58] Blank NPs had no effect on the expression of these genes indicating that the antioxidant activity of blank NPs, on ORAC and DCF-DA assays, is mainly through the direct interaction between peroxyl free radicals and PLGA chains, which inhibit ROS production. The same observation was reported with blank particles on the expression of some genes known to regulate neurogenesis.[51] Interestingly, in normal condition, NPs-Cur can increase the expression of GLRX, TRX, and decrease APOJ genes. In the presence of H_2O_2, NPs-Cur were more efficient than free curcumin to prevent the induction of these genes likely due to higher uptake of NPs-Cur by neuronal cells than free curcumin. This was confirmed with fluorescence microscopy as previously reported.[23] The normalization of the expression of these genes in the presence of PLGA NPs-Cur is in line with their effects on antioxidant pathways.[59,60]

These results are of great interest because the inductions of these genes are well-known to be representative of cellular damages. Indeed, they are upregulated in neuropathological conditions such as in AD.[61] ApoJ, Trx, and Grx levels increased significantly in MCI and AD patients and are correlated with the levels of phosphorylated tau (p-tau),[56,62] while the deletion of REST in the brain is associated with age-related neurodegeneration.[58]

We and others have previously demonstrated that curcumin was taken up by neuronal cells following the treatment of SK-N-SH cells with NPs-Cur.[23] However, the demonstration of the uptake of PLGA NPs by neuronal cells is challenging. By using fluorescence microscopy, we demonstrated that the photostable PLGA-Lumogen NPs were highly taken up by neuronal cells. These results indicate that NPs-Cur are taken up in a concentration-dependent manner by neuronal cells and could release curcumin inside cells, while PLGA is degraded into lactide and glycolide acid and eliminated via the Krebs cycle. NPs uptake could be caveole- or clathrin-mediated endocytosis.[63−65]

In conclusion, our study demonstrated that curcumin-loaded nanoparticles prolonged and enhanced the antioxidant, anti-inflammatory activity of curcumin while suppressing the Akt and Tau phosphorylation and gene upregulation under oxidative stress conditions. We have also demonstrated the role of the choice of the polymer composition in drug-loaded formulation. Indeed, the ratio of lactic/glycolic acid influences the physicochemical properties of the nanoparticles that will consequently impact on the *in vivo* properties by modulating the entrapment efficiency and the *in vitro* drug release. To summarize, curcumin-loaded PLGA 50:50 formulations are likely to have a greater potential for pharmacological applications and seem to be the best compromise in being used to treat neurodegenerative disorders such as AD.

AUTHOR INFORMATION

Corresponding Author

*E-mail: Charles.Ramassamy@iaf.inrs.ca. Phone: 1- 450 687-5010.

Notes

The authors declare no competing financial interest.

ACKNOWLEDGMENTS

Financial support was obtained from Natural Sciences and Engineering Research Council (to C.R., NSERC), from Louise and André Charron Chair in Alzheimer's disease, and Foundation Universitaire Armand-Frappier-INRS (C.R.) and Conseil Régional de Lorraine (O.J.).

REFERENCES

(1) Carter, M. D.; Simms, G. A.; Weaver, D. F. The development of new therapeutics for Alzheimer's disease. *Clin. Pharmacol. Ther.* **2010**, *88* (4), 475−86.

(2) Ferri, C. P.; Prince, M.; Brayne, C.; Brodaty, H.; Fratiglioni, L.; Ganguli, M.; Hall, K.; Hasegawa, K.; Hendrie, H.; Huang, Y.; Jorm, A.; Mathers, C.; Menezes, P. R.; Rimmer, E.; Scazufca, M. Alzheimer's Disease, I. Global prevalence of dementia: a Delphi consensus study. *Lancet* **2005**, *366* (9503), 2112−7.

(3) Russ, T. C.; Morling, J. R. Cholinesterase inhibitors for mild cognitive impairment. *Cochrane Database Syst. Rev.* **2012**, *9*, CD009132.

(4) Giacobini, E. Cholinesterase inhibitor therapy stabilizes symptoms of Alzheimer disease. *Alzheimer Dis. Assoc. Disord.* **2000**, *14* (Suppl 1), S3−10.

(5) Krstic, D.; Knuesel, I. Deciphering the mechanism underlying late-onset Alzheimer disease. *Nat. Rev. Neurol.* **2012**, *9* (1), 25−34.

(6) Caldeira, G. L.; Ferreira, I. L.; Rego, A. C. Impaired transcription in Alzheimer's disease: key role in mitochondrial dysfunction and oxidative stress. *J. Alzheimers Dis.* **2013**, *34* (1), 115−31.

(7) Singh, M.; Dang, T. N.; Arseneault, M.; Ramassamy, C. Role of by-products of lipid oxidation in Alzheimer's disease brain: a focus on acrolein. *J. Alzheimers Dis.* **2010**, *21* (3), 741−56.

(8) Christen, Y. Oxidative stress and Alzheimer disease. *Am. J. Clin. Nutr.* **2000**, *71* (2), 621S−629S.

(9) Sultana, R.; Butterfield, D. A. Oxidative modification of brain proteins in Alzheimer's disease: perspective on future studies based on results of redox proteomics studies. *J. Alzheimers Dis.* **2013**, *33* (Suppl 1), S243−51.

DOI: 10.1021/acs.molpharmaceut.5b00611
Mol. Pharmaceutics 2016, 13, 391−403

(10) Smith, M. A.; Zhu, X.; Tabaton, M.; Liu, G.; McKeel, D. W., Jr.; Cohen, M. L.; Wang, X.; Siedlak, S. L.; Dwyer, B. E.; Hayashi, T.; Nakamura, M.; Nunomura, A.; Perry, G. Increased iron and free radical generation in preclinical Alzheimer disease and mild cognitive impairment. *J. Alzheimers Dis.* **2010**, *19* (1), 363−72.
(11) Hudson, G.; Sims, R.; Harold, D.; Chapman, J.; Hollingworth, P.; Gerrish, A.; Russo, G.; Hamshere, M.; Moskvina, V.; Jones, N.; Thomas, C.; Stretton, A.; Holmans, P. A.; O'Donovan, M. C.; Owen, M. J.; Williams, J.; Chinnery, P. F. No consistent evidence for association between mtDNA variants and Alzheimer disease. *Neurology* **2012**, *78* (14), 1038−42.
(12) Belkacemi, A.; Ramassamy, C. Time sequence of oxidative stress in the brain from transgenic mouse models of Alzheimer's disease related to the amyloid-beta cascade. *Free Radical Biol. Med.* **2012**, *52* (3), 593−600.
(13) Aggarwal, B. B.; Sundaram, C.; Malani, N.; Ichikawa, H. Curcumin: the Indian solid gold. *Adv. Exp. Med. Biol.* **2007**, *595*, 1−75.
(14) Ringman, J. M.; Frautschy, S. A.; Teng, E.; Begum, A. N.; Bardens, J.; Beigi, M.; Gylys, K. H.; Badmaev, V.; Heath, D. D.; Apostolova, L. G.; Porter, V.; Vanek, Z.; Marshall, G. A.; Hellemann, G.; Sugar, C.; Masterman, D. L.; Montine, T. J.; Cummings, J. L.; Cole, G. M. Oral curcumin for Alzheimer's disease: tolerability and efficacy in a 24-week randomized, double blind, placebo-controlled study. *Alzheimer's Res. Ther.* **2012**, *4*, (5), 43. DOI: 10.1186/alzrt146.
(15) Ryu, E. K.; Choe, Y. S.; Lee, K. H.; Choi, Y.; Kim, B. T. Curcumin and dehydrozingerone derivatives: synthesis, radiolabeling, and evaluation for beta-amyloid plaque imaging. *J. Med. Chem.* **2006**, *49* (20), 6111−9.
(16) Begum, A. N.; Jones, M. R.; Lim, G. P.; Morihara, T.; Kim, P.; Heath, D. D.; Rock, C. L.; Pruitt, M. A.; Yang, F.; Hudspeth, B.; Hu, S.; Faull, K. F.; Teter, B.; Cole, G. M.; Frautschy, S. A. Curcumin structure-function, bioavailability, and efficacy in models of neuroinflammation and Alzheimer's disease. *J. Pharmacol. Exp. Ther.* **2008**, *326* (1), 196−208.
(17) Baum, L.; Ng, A. Curcumin interaction with copper and iron suggests one possible mechanism of action in Alzheimer's disease animal models. *J. Alzheimers Dis.* **2004**, *6* (4), 367−77.
(18) Belkacemi, A.; Doggui, S.; Dao, L.; Ramassamy, C. Challenges associated with curcumin therapy in Alzheimer disease. *Expert Rev. Mol. Med.* **2011**, *13*, e34.
(19) Doggui, S.; Belkacemi, A.; Paka, G. D.; Perrotte, M.; Pi, R. B.; Ramassamy, C. Curcumin protects neuronal-like cells against acrolein by restoring Akt and redox signaling pathways. *Mol. Nutr. Food Res.* **2013**, *57* (9), 1660−1670.
(20) Dang, T. N.; Arseneault, M.; Zarkovic, N.; Waeg, G.; Ramassamy, C. Molecular regulations induced by acrolein in neuroblastoma SK-N-SH cells: relevance to Alzheimer's disease. *J. Alzheimers Dis.* **2010**, *21* (4), 1197−216.
(21) Thanh Nam, D.; Arseneault, M.; Murthy, V.; Ramassamy, C. Potential role of acrolein in neurodegeneration and in Alzheimer's disease. *Curr. Mol. Pharmacol* **2010**, *3* (2), 66−78.
(22) Baum, L.; Lam, C. W.; Cheung, S. K.; Kwok, T.; Lui, V.; Tsoh, J.; Lam, L.; Leung, V.; Hui, E.; Ng, C.; Woo, J.; Chiu, H. F.; Goggins, W. B.; Zee, B. C.; Cheng, K. F.; Fong, C. Y.; Wong, A.; Mok, H.; Chow, M. S.; Ho, P. C.; Ip, S. P.; Ho, C. S.; Yu, X. W.; Lai, C. Y.; Chan, M. H.; Szeto, S.; Chan, I. H.; Mok, V. Six-month randomized, placebo-controlled, double-blind, pilot clinical trial of curcumin in patients with Alzheimer disease. *J. Clin. Psychopharmacol.* **2008**, *28* (1), 110−3.
(23) Doggui, S.; Sahni, J. K.; Arseneault, M.; Dao, L.; Ramassamy, C. Neuronal uptake and neuroprotective effect of curcumin-loaded PLGA nanoparticles on the human SK-N-SH cell line. *J. Alzheimers Dis.* **2012**, *30* (2), 377−92.
(24) Jain, R. A. The manufacturing techniques of various drug loaded biodegradable poly(lactide-co-glycolide) (PLGA) devices. *Biomaterials* **2000**, *21* (23), 2475−90.
(25) Makadia, H. K.; Siegel, S. J. Poly Lactic-co-Glycolic Acid (PLGA) as Biodegradable Controlled Drug Delivery Carrier. *Polymers (Basel, Switz.)* **2011**, *3* (3), 1377−1397.
(26) Bala, I.; Hariharan, S.; Kumar, M. N. PLGA nanoparticles in drug delivery: the state of the art. *Crit. Rev. Ther. Drug Carrier Syst.* **2004**, *21* (5), 387−422.
(27) Trofymchuk, K.; Reisch, A.; Shulov, I.; Mely, Y.; Klymchenko, A. S. Tuning the color and photostability of perylene diimides inside polymer nanoparticles: towards biodegradable substitutes of quantum dots. *Nanoscale* **2014**, *6* (21), 12934−12942.
(28) Rigaux, G.; Roullin, V. G.; Cadiou, C.; Portefaix, C.; Van Gulick, L.; Baeuf, G.; Andry, M. C.; Hoeffel, C.; Vander Elst, L.; Laurent, S.; Muller, R.; Molinari, M.; Chuburu, F. A new magnetic resonance imaging contrast agent loaded into poly(lacide-co-glycolide) nanoparticles for long-term detection of tumors. *Nanotechnology* **2014**, *25* (44), 445103.
(29) Sankar, M. Binding and stability of curcumin in presence of bovine serum albumin. *J. Surface Sci. Technol.* **2007**, *23* (3−4), 91−110.
(30) Gu, L.; Zhao, M.; Li, W.; You, L.; Wang, J.; Wang, H.; Ren, J. Chemical and cellular antioxidant activity of two novel peptides designed based on glutathione structure. *Food Chem. Toxicol.* **2012**, *50* (11), 4085−91.
(31) Ou, B.; Hampsch-Woodill, M.; Prior, R. L. Development and validation of an improved oxygen radical absorbance capacity assay using fluorescein as the fluorescent probe. *J. Agric. Food Chem.* **2001**, *49* (10), 4619−26.
(32) Davalos, A.; Gomez-Cordoves, C.; Bartolome, B. Extending applicability of the oxygen radical absorbance capacity (ORAC-fluorescein) assay. *J. Agric. Food Chem.* **2004**, *52* (1), 48−54.
(33) Peirson, S. N.; Butler, J. N.; Foster, R. G. Experimental validation of novel and conventional approaches to quantitative real-time PCR data analysis. *Nucleic Acids Res.* **2003**, *31* (14), 73e.
(34) Boeuf, G.; Roullin, G. V.; Moreau, J.; Van Gulick, L.; Zambrano Pineda, N.; Terryn, C.; Ploton, D.; Andry, M. C.; Chuburu, F.; Dukic, S.; Molinari, M.; Lemercier, G. Encapsulated Ruthenium(II) Complexes in Biocompatible Poly(D,L-lactide-co-glycolide) Nanoparticles for Application in Photodynamic Therapy. *ChemPlusChem* **2014**, *79* (1), 171−180.
(35) Roullin, V. G.; Callewaert, M.; Molinari, M.; Delavoie, F.; Seconde, A.; Andry, M. C. Optimised NSAIDs-loaded Biocompatible Nanoparticles. *Nano-Micro Lett.* **2010**, *2* (4), 247−255.
(36) Cao, G.; Alessio, H. M.; Cutler, R. G. Oxygen-radical absorbance capacity assay for antioxidants. *Free Radical Biol. Med.* **1993**, *14* (3), 303−11.
(37) Candelario-Jalil, E.; Yang, Y.; Rosenberg, G. A. Diverse roles of matrix metalloproteinases and tissue inhibitors of metalloproteinases in neuroinflammation and cerebral ischemia. *Neuroscience* **2009**, *158* (3), 983−94.
(38) Chuang, Y.-Y.; Chen, Y.; Gadisetti; Chandramouli, V. R.; Cook, J. A.; Coffin, D.; Tsai, M. H.; DeGraff, W.; Yan, H.; Zhao, S.; Russo, A.; Liu, E. T.; Mitchell, J. B. Gene Expression after Treatment with Hydrogen Peroxide, Menadione, or t-Butyl Hydroperoxide in Breast Cancer Cells. *Cancer Res.* **2002**, *62*, 6246−6254.
(39) Tsai, Y. M.; Chien, C. F.; Lin, L. C.; Tsai, T. H. Curcumin and its nano-formulation: The kinetics of tissue distribution and blood-brain barrier penetration. *Int. J. Pharm.* **2011**, *416* (1), 331−338.
(40) Lockman, P. R.; Mumper, R. J.; Khan, M. A.; Allen, D. D. Nanoparticle technology for drug delivery across the blood-brain barrier. *Drug Dev. Ind. Pharm.* **2002**, *28* (1), 1−13.
(41) Hill, L. E.; Taylor, T. M.; Gomes, C. Antimicrobial efficacy of poly (DL-lactide-co-glycolide) (PLGA) nanoparticles with entrapped cinnamon bark extract against Listeria monocytogenes and Salmonella typhimurium. *J. Food Sci.* **2013**, *78* (4), N626−32.
(42) Bisht, S.; Feldmann, G.; Soni, S.; Ravi, R.; Karikar, C.; Maitra, A.; Maitra, A. Polymeric nanoparticle-encapsulated curcumin ("nanocurcumin"): a novel strategy for human cancer therapy. *J. Nanobiotechnol.* **2007**, *5*, 3.
(43) Xie, X.; Tao, Q.; Zou, Y.; Zhang, F.; Guo, M.; Wang, Y.; Wang, H.; Zhou, Q.; Yu, S. PLGA nanoparticles improve the oral bioavailability of curcumin in rats: characterizations and mechanisms. *J. Agric. Food Chem.* **2011**, *59* (17), 9280−9.

DOI: 10.1021/acs.molpharmaceut.5b00611
Mol. Pharmaceutics 2016, 13, 391−403

(44) Chereddy, K. K.; Coco, R.; Memvanga, P. B.; Ucakar, B.; des Rieux, A.; Vandermeulen, G.; Preat, V. Combined effect of PLGA and curcumin on wound healing activity. *J. Controlled Release* **2013**, *171* (2), 208−15.
(45) Loo, J. S.; Ooi, C. P.; Boey, F. Y. Degradation of poly(lactide-co-glycolide) (PLGA) and poly(L-lactide) (PLLA) by electron beam radiation. *Biomaterials* **2005**, *26* (12), 1359−67.
(46) Mattson, M. P. Pathways towards and away from Alzheimer's disease. *Nature* **2004**, *430* (7000), 631−9.
(47) Buhrmann, C.; Mobasheri, A.; Busch, F.; Aldinger, C.; Stahlmann, R.; Montaseri, A.; Shakibaei, M. Curcumin modulates nuclear factor kappaB (NF-kappaB)-mediated inflammation in human tenocytes in vitro: role of the phosphatidylinositol 3-kinase/Akt pathway. *J. Biol. Chem.* **2011**, *286* (32), 28556−66.
(48) Jimenez, S.; Torres, M.; Vizuete, M.; Sanchez-Varo, R.; Sanchez-Mejias, E.; Trujillo-Estrada, L.; Carmona-Cuenca, I.; Caballero, C.; Ruano, D.; Gutierrez, A.; Vitorica, J. Age-dependent accumulation of soluble amyloid beta (Abeta) oligomers reverses the neuroprotective effect of soluble amyloid precursor protein-alpha (sAPP(alpha)) by modulating phosphatidylinositol 3-kinase (PI3K)/Akt-GSK-3beta pathway in Alzheimer mouse model. *J. Biol. Chem.* **2011**, *286* (21), 18414−25.
(49) Feng, Y.; Xia, Y.; Yu, G.; Shu, X.; Ge, H.; Zeng, K.; Wang, J.; Wang, X. Cleavage of GSK-3beta by calpain counteracts the inhibitory effect of Ser9 phosphorylation on GSK-3beta activity induced by H(2)O(2). *J. Neurochem.* **2013**, *126* (2), 234−42.
(50) Ma, Q. L.; Zuo, X.; Yang, F.; Ubeda, O. J.; Gant, D. J.; Alaverdyan, M.; Teng, E.; Hu, S.; Chen, P. P.; Maiti, P.; Teter, B.; Cole, G. M.; Frautschy, S. A. Curcumin suppresses soluble tau dimers and corrects molecular chaperone, synaptic, and behavioral deficits in aged human tau transgenic mice. *J. Biol. Chem.* **2013**, *288* (6), 4056−65.
(51) Tiwari, S. K.; Agarwal, S.; Seth, B.; Yadav, A.; Nair, S.; Bhatnagar, P.; Karmakar, M.; Kumari, M.; Chauhan, L. K.; Patel, D. K.; Srivastava, V.; Singh, D.; Gupta, S. K.; Tripathi, A.; Chaturvedi, R. K.; Gupta, K. C. Curcumin-loaded nanoparticles potently induce adult neurogenesis and reverse cognitive deficits in Alzheimer's disease model via canonical Wnt/beta-catenin pathway. *ACS Nano* **2014**, *8* (1), 76−103.
(52) Trougakos, I. P.; Gonos, E. S. Regulation of clusterin/apolipoprotein J, a functional homologue to the small heat shock proteins, by oxidative stress in ageing and age-related diseases. *Free Radical Res.* **2006**, *40* (12), 1324−34.
(53) Zhu, G.; Barrie, A.; Ebert, C.; Rosenberg, M. E.; Witte, D. P.; Harmony, J. A. K. Clusterin gene locus structure and function in development, homeostasis, and tissue injury. In *Clusterin in Normal Brain Functions and during Neurodegeneration*; RG Landes Company, 1999; pp 1−16.
(54) Ramassamy, C.; Averill, D.; Beffert, U.; Bastianetto, S.; Theroux, L.; Lussier-Cacan, S.; Cohn, J. S.; Christen, Y.; Davignon, J.; Quirion, R.; Poirier, J. Oxidative damage and protection by antioxidants in the frontal cortex of Alzheimer's disease is related to the apolipoprotein E genotype. *Free Radical Biol. Med.* **1999**, *27* (5−6), 544−53.
(55) Poirier, J.; Miron, J.; Picard, C.; Gormley, P.; Theroux, L.; Breitner, J.; Dea, D. Apolipoprotein E and lipid homeostasis in the etiology and treatment of sporadic Alzheimer's disease. *Neurobiol. Aging* **2014**, *35* (Suppl 2), S3−10.
(56) Arodin, L.; Lamparter, H.; Karlsson, H.; Nennesmo, I.; Bjornstedt, M.; Schroder, J.; Fernandes, A. P. Alteration of thioredoxin and glutaredoxin in the progression of Alzheimer's disease. *J. Alzheimers Dis.* **2014**, *39* (4), 787−97.
(57) Mahmood, D. F.; Abderrazak, A.; El Hadri, K.; Simmet, T.; Rouis, M. The thioredoxin system as a therapeutic target in human health and disease. *Antioxid. Redox Signaling* **2013**, *19* (11), 1266−303.
(58) Lu, T.; Aron, L.; Zullo, J.; Pan, Y.; Kim, H.; Chen, Y.; Yang, T. H.; Kim, H. M.; Drake, D.; Liu, X. S.; Bennett, D. A.; Colaiacovo, M. P.; Yankner, B. A. REST and stress resistance in ageing and Alzheimer's disease. *Nature* **2014**, *507* (7493), 448−54.
(59) Lee, Y.; Aono, M.; Laskowitz, D.; Warner, D. S.; Pearlstein, R. D. Apolipoprotein E protects against oxidative stress in mixed neuronal-glial cell cultures by reducing glutamate toxicity. *Neurochem. Int.* **2004**, *44* (2), 107−18.
(60) Ito, J. I.; Nagayasu, Y.; Ogawa, T.; Okihara, H.; Michikawa, M. Biochemical properties in membrane of rat astrocytes under oxidative stress. *Brain Res.* **2015**, *1615*, 1.
(61) Desikan, R. S.; Thompson, W. K.; Holland, D.; Hess, C. P.; Brewer, J. B.; Zetterberg, H.; Blennow, K.; Andreassen, O. A.; McEvoy, L. K.; Hyman, B. T.; Dale, A. M. The role of clusterin in amyloid-beta-associated neurodegeneration. *JAMA Neurol* **2014**, *71* (2), 180−7.
(62) Mullan, G. M.; McEneny, J.; Fuchs, M.; McMaster, C.; Todd, S.; McGuinness, B.; Henry, M.; Passmore, A. P.; Young, I. S.; Johnston, J. A. Plasma clusterin levels and the rs11136000 genotype in individuals with mild cognitive impairment and Alzheimer's disease. *Curr. Alzheimer Res.* **2013**, *10* (9), 973−8.
(63) Hu, K.; Shi, Y.; Jiang, W.; Han, J.; Huang, S.; Jiang, X. Lactoferrin conjugated PEG-PLGA nanoparticles for brain delivery: preparation, characterization and efficacy in Parkinson's disease. *Int. J. Pharm.* **2011**, *415* (1−2), 273−83.
(64) Hillaireau, H.; Couvreur, P. Nanocarriers' entry into the cell: relevance to drug delivery. *Cell. Mol. Life Sci.* **2009**, *66* (17), 2873−96.
(65) Safar, R.; Ronzani, C.; Diab, R.; Chevrier, J.; Bensoussan, D.; Grandemange, S.; Le Faou, A.; Rihn, B. H.; Joubert, O. Human monocyte response to S-nitrosoglutathione-loaded nanoparticles: uptake, viability, and transcriptome. *Mol. Pharmaceutics* **2015**, *12* (2), 554−61.

DOI: 10.1021/acs.molpharmaceut.5b00611
Mol. Pharmaceutics 2016, 13, 391−403